Geochemical Perspectives Letters

Tight bounds on missing late veneer in early Archean peridotite from triple oxygen isotopes

S.T.M. Peters[1*], M.B. Fischer[1,2], A. Pack[1], K. Szilas[3], P.W.U. Appel[4], C. Münker[5], L. Dallai[6], C.S. Marien[5]

OPEN ACCESS
doi: 10.7185/geochemlet.2120

Abstract

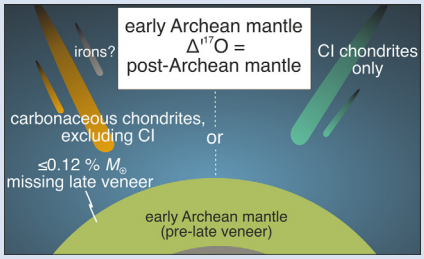

Oxygen isotopes provide a unique possibility to study Earth's late accretion phase from a lithophile element perspective, because most carbonaceous chondrites – meteorites that likely resemble the composition of the terrestrial late veneer – have markedly different $\Delta'^{17}O$ values than the silicate Earth. Ultramafic rocks in the early Archean assemblage of southwest Greenland have not incorporated the full amount of late accreted materials, and therefore possibly record the $\Delta'^{17}O$ of the mantle before late accretion. We measured $^{17}O/^{16}O$ and $^{18}O/^{16}O$ ratios of olivine from these ultramafic rocks and compared them with olivine from post-Archean mantle peridotite. A missing late veneer component was not resolved. The missing component from the early Archean mantle is therefore restricted to ≤0.12 % of Earth's mass ($M_\oplus$) for most carbonaceous chondrite-like materials, unless the missing component resembles CI chondrites – the only carbonaceous chondrites with $\Delta'^{17}O$ values similar to those of the silicate Earth. If the early Archean mantle had incorporated 60 % late veneer, the overall late accreted mass would be restricted to ≤0.3 % $M_\oplus$ for most types of carbonaceous chondrites, with a more massive late veneer only possible for CI-like chondrites.

Received 7 March 2021 | Accepted 18 June 2021 | Published 1 September 2021

Introduction

Missing late veneer in early Archean mantle domains. Earth formed by the accretion of rocky materials in a protoplanetary disk. The final ~0.5 % of these materials escaped metal-silicate equilibrium during core formation processes, and are commonly referred to as the late veneer (Walker, 2009). The composition of these late accreted materials is interesting to study, because they possibly contributed a large portion of volatile elements and water to the Earth's mass (Wang and Becker, 2013; Braukmüller *et al.*, 2019).

Based on platinum and tungsten isotope work, it was proposed that some Archean mantle domains did not incorporate the full amount of late veneer (*e.g.*, Willbold *et al.*, 2011; Creech *et al.*, 2017). Such mantle domains could then provide unique windows into the final stages of Earth's accretion and its earliest evolution. An unambiguous pre-late veneer signal is present in ultramafic enclaves that are entrained in the Eoarchean Itsaq Gneiss Complex and Mesoarchean Fiskefjord region of southwest Greenland. These rocks show a uniform excess in s-process Ru nuclides compared to r-process Ru nuclides relative to the bulk silicate Earth (Fischer-Gödde *et al.*, 2020). The excess s-process Ru in the ultramafic enclaves is best explained by a deficit in late accreted materials that carried a deficit in s-process Ru. Whereas both carbonaceous and non-carbonaceous chondrite groups carry deficits in s-process Ru, the s-process deficit is only sufficiently large in carbonaceous chondrite groups to potentially account for the observed s-process excess in the ultramafic enclaves, given the concentrations of platinum group elements in the Eoarchean mantle (Fischer-Gödde *et al.*, 2020). This conclusion is important, because it would support a volatile-rich, carbonaceous chondrite-like late veneer, and therewith complement evidence from volatile chalcophile elements in the post-Archean mantle (Wang and Becker, 2013; Braukmüller *et al.*, 2019; Varas-Reus *et al.*, 2019).

Potential of studying triple oxygen isotope ratios. Oxygen stable isotope ratios ($^{17}O/^{16}O$, $^{18}O/^{16}O$) are a unique tool for studying late accretion processes from a lithophile element perspective (Rumble *et al.*, 2013; Valley *et al.*, 2014; Young *et al.*, 2016; Reimink *et al.*, 2018), because bulk asteroids in the Solar System show ~6000 ppm variations in $\Delta'^{17}O$ (Clayton, 1993). This is large compared to the ~5 ppm analytical resolution of state of the art laser fluorination techniques. Henceforth, we use a definition for $\Delta'^{17}O$ with:

1. Georg-August-Universität Göttingen, Geowissenschaftliches Zentrum, Goldschmidtstraße 1, 37077 Göttingen, Germany
2. Max-Planck-Institut für Sonnensystemforschung, Justus-von-Liebig-Weg 3, 37077 Göttingen, Germany
3. University of Copenhagen, Department of Geosciences and Natural Resource Management, Øster Voldgade 10, 1350 København K, Denmark
4. Geological Survey of Denmark and Greenland, Øster Voldgade 10, 1350 København K, Denmark
5. Universität zu Köln, Institut für Geologie und Mineralogie, Zülpicher Str. 49b, 50674 Köln, Germany
6. CNR-Istituto di Geoscienze e Georisorse, Via Moruzzi 1, 56124 Pisa, Italy

* Corresponding author (email: s.peters@geo.uni-goettingen.de)

$$\Delta'^{17}O = 1000\left[1000\ln\left(\frac{\delta^{17}O}{1000}+1\right) - 0.528\times 1000\ln\left(\frac{\delta^{18}O}{1000}+1\right)\right] \quad \text{Eq. 1}$$

Carbonaceous chondrites have lower $\Delta'^{17}O$ values than the silicate Earth, with only CI chondrites having similar but slightly higher $\Delta'^{17}O$ and much higher $\delta^{18}O$ values than the silicate Earth (Clayton, 1993). If the early Archean ultramafic enclaves from southwest Greenland would have been deprived of a late veneer component that resembles most carbonaceous chondrite types (CM, CV, CO, CK, CR, CH, CB chondrites), samples from the early Archean ultramafic enclaves would therefore be expected to have an elevated $\Delta'^{17}O$ compared to the silicate Earth. Only if the ultramafic enclaves would be missing a late veneer component that resembles CI chondrites, would they have a similar or lower $\Delta'^{17}O$ than the silicate Earth. In order to study mass and composition of the missing late veneer component from the early Archean ultramafic enclaves of southwest Greenland, we therefore compared their olivine $\Delta'^{17}O$ values with olivine in post-Archean mantle peridotite.

Samples and Methods

The suite of post-Archean mantle peridotite sample comprises 14 lherzolithic xenoliths that were erupted in Phanerozoic magmas from diverse geological settings, and 1 dunite sample from the Beni Boussera massif (Supplementary Information S-1). The ultramafic enclaves with s-process Ru excess (Fischer-Gödde *et al.*, 2020) that we studied are from two localities within the >3.7 Ga Isua supracrustal belt (ISB), one locality south of the Isua supracrustal belt (SOISB), the ~3.8 Ga Narssaq ultramafic body (NUB), and the ~3.8 Ga Ujaragssuit Nunât ultramafic body (Supplementary Information S-1). The early Archean ultramafic bodies were interpreted either as slivers of residual mantle peridotite, as metamorphosed cumulates from (ultra)mafic magmas, or, for one location, as an ultramafic layered intrusion. We also studied peridotite samples from the Fiskefjord region that are geologically related to the Mesoarchean Seqi peridotite body (Szilas *et al.*, 2015), for which an excess in s-process Ru compared to the silicate Earth was also reported (Fischer-Gödde *et al.*, 2020). Olivine samples were analysed for their triple oxygen isotope compositions ($\delta^{17}O$, $\delta^{18}O$) using laser assisted fluorination protocols (Supplementary Information S-2). All samples were analysed relative to San Carlos olivine, which is considered here to have a $\Delta'^{17}O = -51.8$ ppm relative to VSMOW.

Results

Olivine $\delta^{18}O$ values of the post-Archean mantle peridotite samples are on average $\delta^{18}O = 5.21 \pm 0.08$ ‰ (1 s.d., $n = 15$), which is in good agreement with previous data for olivine in mantle peridotite (*e.g.*, Mattey *et al.*, 1994) (Table S-1). The post-Archean mantle peridotite samples have an average olivine $\Delta'^{17}O$ value of -51.6 ± 2.1 ppm (1 s.d., $n = 15$; Fig. 1a), which is in line with data for mafic and ultramafic rocks from previous studies (Herwartz *et al.*, 2014; Greenwood *et al.*, 2018; Cano *et al.*, 2020). No variations in olivine $\Delta'^{17}O$ values were found for the post-Archean mantle peridotite samples. The peridotite samples from the Archean ultramafic enclaves in the Itsaq Gneiss Complex and Fiskefjord region show a much wider range in olivine $\delta^{18}O$ values ($\delta^{18}O = 2.8$–6.2 ‰) (Table S-2). Olivine $\Delta'^{17}O$ values of the early Archean ultramafic bodies are on average $\Delta'^{17}O = -50.9 \pm 3.2$ ppm (1 s.d., $n = 23$), a value that is indistinguishable from the $\Delta'^{17}O$ value of post-Archean mantle olivine. The early Archean peridotite samples show decreasing olivine $\Delta'^{17}O$ values with increasing $\delta^{18}O$ values (Fig. 1b).

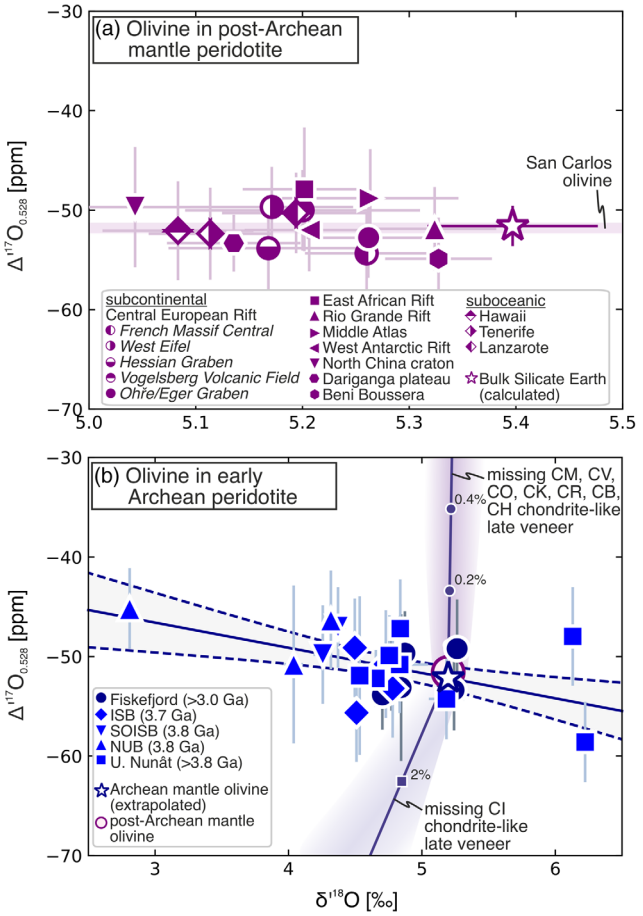

Figure 1 Plots of $\Delta'^{17}O$ *vs.* $\delta'^{18}O$ (±1 s.e.m.) of olivine from ultramafic rocks. **(a)** Olivine in peridotites that were erupted as xenoliths in Phanerozoic magmas and from the Beni Boussera massif, relative to the composition of San Carlos olivine (horizontal line, $\Delta'^{17}O = -51.8$ ppm; Supplementary Information S-2). The composition of the bulk silicate Earth (star) is calculated from the mean olivine compositions from this study ±1 s.d. and is based on −0.2 ‰ fractionation in $\delta^{18}O$ and a θ value of 0.53 for fractionation between olivine and bulk peridotite. **(b)** Olivine from early Archean ultramafic enclaves with excess s-process Ru (Fischer-Gödde *et al.*, 2020). The curve corresponds to a linear fit ±1 s.d. through the Archean peridotite data in $\delta^{17}O$ *versus* $\delta^{18}O$ space and is used to extrapolate the compositions of the samples, which were in part altered by fluid-rock reactions, to the $\Delta'^{17}O$ of pristine olivine in the early Archean mantle with $\delta^{18}O = 5.21$ ‰ (star). Shadowed fields correspond to calculated olivine compositions if carbonaceous chondrites would be missing from the ultramafic enclaves, considering all carbonaceous chondrite meteorites for which data are available in the Meteoritical Bulletin Database as possible end member compositions for the late veneer (Table S-3). Curves are shown for missing late veneer with the average composition of CM, CV, CO, CK, CR, CH, CB chondrites and the average composition of CI chondrites, respectively, with the percentages of missing late veneer indicated relative to the mass of the Earth.

Discussion

Effects of fluid-rock reactions. Olivine $\delta^{18}O$ values of the early Archean peridotites predominantly deviate towards lower values

compared to post-Archean mantle olivine. We reported similarly low and variable olivine $\delta^{18}O$ values for a >2.7 Ga peridotite body that is entrained in the Kuummiut terrane in southeast Greenland, for which the low and variable $\delta^{18}O$ values reflect the effects of fluid-rock reactions that were followed by dehydration of the peridotitic protoliths at high grade metamorphic conditions (Peters *et al.*, 2020). Likewise, we suggest that the ultramafic enclaves in the Itsaq Gneiss Complex and Fiskefjord region experienced hydration and dehydration events during their metamorphic history that modified their primary olivine $\delta^{18}O$ values, a process that is likely common for ultramafic rocks in Archean high grade metamorphic terranes (Nishio *et al.*, 2019) (Supplementary Information S-1). Fluid-rock reactions cannot only have shifted the $\delta^{18}O$ values of the Archean peridotite samples, but may also have altered the $\Delta'^{17}O$ values of the peridotite samples (*e.g.*, Sengupta and Pack, 2018). In order to obtain the $\Delta'^{17}O$ value of pristine olivine in the ultramafic rocks before they interacted with fluids, we extrapolated the measured $\Delta'^{17}O$ values to the $\delta^{18}O$ value of typical mantle olivine (this study; $\delta^{18}O = 5.21$ ‰) (Fig. 1b). The extrapolated $\Delta'^{17}O$ value of pristine olivine in the early Archean mantle is -52.3 ± 1.7 ppm (1 s.d.); a value that is only 1.4 ppm lower than the average $\Delta'^{17}O$ of the uncorrected data.

Implications for missing late veneer. The suggested $\Delta'^{17}O$ value of pristine olivine in the early Archean ultramafic rocks is indistinguishable from the mean $\Delta'^{17}O$ value of olivine in post-Archean mantle peridotite (Fig. 1b). A pre-late veneer signal in the Archean ultramafic enclaves is thus not resolved with respect to oxygen isotopes. This conclusion corroborates earlier results from a laser fluorination study on the Acasta Gneiss Complex and Isua supracrustal belt (Rumble *et al.*, 2013), and lower resolution SIMS data for the Jack Hills zircons, as well as zircons from the Acasta Gneiss Complex and (Valley *et al.*, 2014; Reimink *et al.*, 2018). Using the new data, we calculated the uppermost likely limits for missing late veneer from the Itsaq Gneiss Complex and Fiskefjord mantle, assuming the compositions of carbonaceous chondrite groups as the missing components (*c.f.* Fischer-Gödde *et al.*, 2020). In general, and by definition, the compositions of the mantle before the late veneer (hereafter 'pre-late veneer mantle'; PLVM), the bulk silicate Earth and the late veneer plot on a mixing line in $\delta^{17}O$ *versus* $\delta^{18}O$ space. The slope m and intercept i of this mixing line are given by the $\delta^{17}O$ and $\delta^{18}O$ values of the bulk silicate Earth and the composition of the late veneer. In $\delta'^{17}O$ *versus* $\delta'^{18}O$ space, the composition of the pre-late veneer mantle also plots on a line with slope 0.528 and intercept $\Delta'^{17}O$ that equals the value for the pre-late veneer mantle. The point of intersection of the two relations in $\delta'^{17}O$ *versus* $\delta'^{18}O$ space is given by:

$$0.528\delta'^{18}O_{PLVM} + \frac{\Delta'^{17}O_{PLVM}}{1000} = 1000 \ln\left[me^{\frac{\delta'^{18}O_{PLVM}}{1000}} - m + \frac{i}{1000} + 1\right] \quad \text{Eq. 2}$$

and can be approximated with the Newton-Raphson method. The intersection δ values then allow determining the oxygen atom fraction of missing late veneer from the pre-late veneer mantle (Supplementary Information S-4).

Based on Equation 2 we modelled possible masses of missing late veneer if carbonaceous chondrite groups would be missing from the Itsaq Gneiss Complex and Fiskefjord mantle, using a Monte Carlo approach (Fig. 2). In each Monte Carlo run, the end member composition of the late veneer was selected by randomly sampling a meteorite composition from the carbonaceous chondrite groups of interest, *i.e.* each meteorite specimen from a given selection of carbonaceous chondrites was considered equally likely to represent a possible end member composition of the late veneer (Table S-3). We adopted concentrations in the mixing calculations of 46.5 wt. % oxygen in carbonaceous chondrites and 44.33 wt. % oxygen in the terrestrial mantle (Palme and O'Neill, 2003). In the simulations, the $\Delta'^{17}O$ values for the bulk silicate Earth and the pre-late veneer mantle were sampled from normally distributed populations that are described by the mean values and standard deviations for post-Archean mantle peridotite and the extrapolated $\Delta'^{17}O$ value for pristine olivine in early Archean peridotite from this

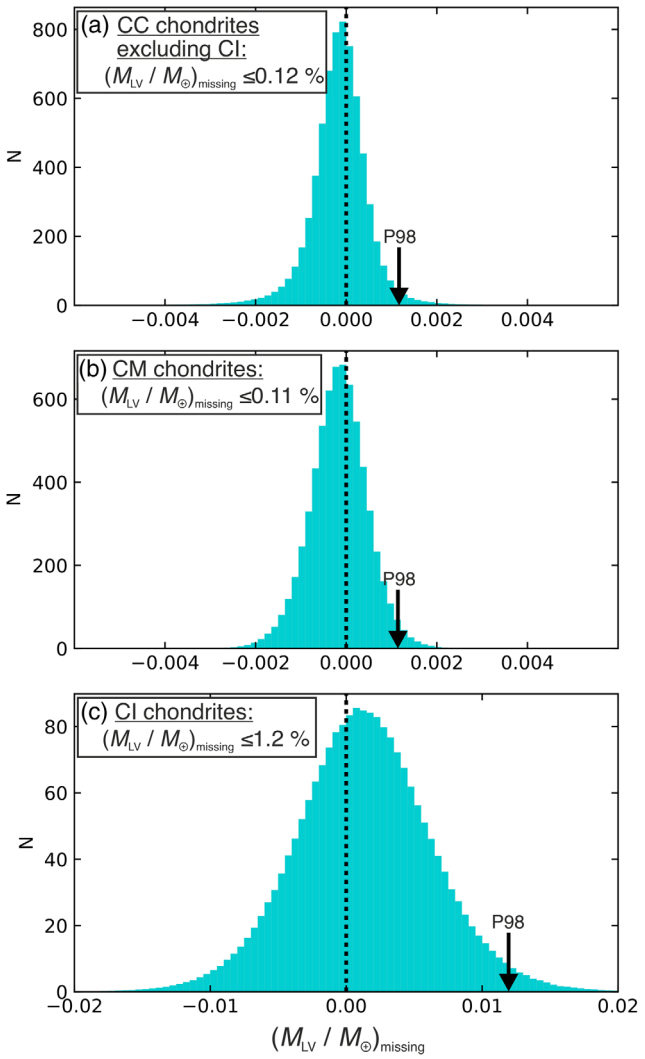

Figure 2 Missing late veneer from the Itsaq Gneiss Complex and Fiskefjord mantle relative to the mass of the Earth, $(M_{LV}/M_{\oplus})_{missing}$, calculated from the data in this study and from available triple oxygen isotope data for carbonaceous chondrites (Monte Carlo simulation; 10^6 runs). End member compositions of the late veneer were sampled randomly for given chondrite groups from a compilation of all meteorite data that are available in the Meteoritical Bulletin Database (Table S-3). The $\delta^{18}O$ value of the silicate Earth was considered to be 0.2 ‰ higher than olivine in mantle peridotite from this study, *i.e.* $\delta^{18}O_{BSE} = 5.41$ ‰. The 97.72nd percentile (P98) of the outcomes are shown by arrows and are given in the panel headings as percentages; and are considered uppermost bounds for missing late veneer. Outcomes with negative values correspond to hypothetical scenarios in which the Itsaq Gneiss Complex and Fiskefjord mantle contain excess late veneer. Dotted lines show outcomes where $(M_{LV}/M_{\oplus})_{missing} = 0$. **(a)** Missing carbonaceous chondrites, excluding CI chondrites. **(b)** Missing CM chondrites only. **(c)** Missing CI chondrites only.

study, respectively. We consider the 97.72nd percentile of the outcomes of the simulations as the uppermost likely values for the missing late veneer. These uppermost values correspond to a missing late veneer component relative to the Earth's mass ($M_\oplus$) of ≤0.12 % $M_\oplus$ if the missing component would resemble CM, CV, CO, CK, CR, CH, CB, but not CI chondrites (Fig. 2a); ≤0.11 % $M_\oplus$ if the missing component would resemble only CM chondrites (Fig. 2b); and ≤1.2 % $M_\oplus$ if the missing component would resemble CI chondrites (Fig. 2c).

Our modelling results have implications for the materials that comprised Earth's late veneer. Fischer-Gödde *et al.* (2020) estimated based on their Ru isotope data that a late veneer component of up to 0.3 % $M_\oplus$ of carbonaceous chondrite-like materials could be missing from the Itsaq Gneiss Complex and Fiskefjord mantle, and favoured CM chondrites as the missing component. The oxygen isotope data, in contrast, imply that only a much smaller component of carbonaceous chondrites (≤0.12 % $M_\oplus$) can possibly be missing from the early Archean ultramafic enclaves with respect to oxygen, unless this component comprises CI chondrites. We propose two end member scenarios that best reconcile the triple oxygen isotope data with the available Ru isotope data. In one end member scenario, the missing late veneer component indeed resembles CM chondrites with the equivalent mass of ≤0.11 % $M_\oplus$ (Fig. 2b). This scenario implies that the early Archean mantle had incorporated more than *ca.* >86 % late veneer with respect to lithophile elements, which agrees with some estimates from the concentrations of highly siderophile elements in the early Archean mantle (van de Löcht *et al.*, 2018), but not with others (Dale *et al.*, 2017). The missing CM chondrite-like component was possibly complemented by a missing component of carbonaceous group iron meteorite-like materials, *e.g.*, materials similar to the IID and IVA irons that have comparable Ru isotope compositions compared to carbonaceous chondrites (Fischer-Gödde and Kleine, 2017) and high Ru concentrations, but are deficient in O. This scenario is also consistent with highly siderophile element concentrations and $^{187}Os/^{188}Os$ ratios in lunar impact rocks and in the upper mantle (Fischer-Gödde and Becker, 2012). In the second end member scenario, the missing late veneer component resembles the composition of CI chondrites (Fig. 2c). This scenario is feasible only if the s-process Ru deficit in CI chondrites is greater than was considered in the modelling by Fischer-Gödde *et al.* (2020). We consider this a reasonable suggestion, because the Ru isotope composition of CI chondrites is constrained at present by a single meteorite specimen only, whereas other carbonaceous chondrite groups show internal Ru isotope variations (Fischer-Gödde and Kleine, 2017).

The discussion of our data thus far concerns the mass and composition of a late veneer component that can possibly be *missing* from the early Archean mantle. It can be assumed instead that the early Archean mantle was deficient in 40 % late accreted materials (Dale *et al.*, 2017). Following this line of logic, the triple oxygen isotope data imply a maximum late accreted mass of ≤0.3 % $M_\oplus$ for CM, CV, CO, CK, CR, CH, CB chondrites; and ≤3 % $M_\oplus$ CI chondrites. In conjunction with the absolute concentrations of highly siderophile elements in the post-Archean mantle, this conclusion would imply that the late veneer contained abundant CI-like materials; a scenario that agrees well with volatile element patterns (Braukmüller *et al.*, 2019) and the Se isotope composition of the post-Archean mantle (Varas-Reus *et al.*, 2019).

Acknowledgements

We thank Jesse Reimink and an anonymous reviewer for constructive feedback on the manuscript, and Helen Williams for editorial handling. Some of the post-Archean peridotite samples were collected in the field by Gerhard Wörner, Tsegaye Abebe Adhana, Qunke Xia, and Yuliya Kochergina. KS acknowledges grant CF18-0090 from the Carlsberg Foundation for field work; CM and CMA acknowledge funding by DFG project Mu 1406/18 within SPP 1833.

Editor: Helen Williams

Additional Information

Supplementary Information accompanies this letter at https://www.geochemicalperspectivesletters.org/article2120.

Cite this letter as: Peters, S.T.M., Fischer, M.B., Pack, A., Szilas, K., Appel, P.W.U., Münker, C., Dallai, L., Marien, C.S. (2021) Tight bounds on missing late veneer in early Archean peridotite from triple oxygen isotopes. *Geochem. Persp. Let.* 18, 27–31.

References

Braukmüller, N., Wombacher, F., Funk, C., Münker, C. (2019) Earth's volatile element depletion pattern inherited from a carbonaceous chondrite-like source. *Nature Geoscience* 12, 564–568.

Cano, E.J., Sharp, Z.D., Shearer, C.K. (2020) Distinct oxygen isotope compositions of the Earth and Moon. *Nature Geoscience* 13, 270–274.

Clayton, R.N. (1993) Oxygen isotopes in meteorites. *Annual Review of Earth and Planetary Sciences* 21, 115–149.

Creech, J.B., Baker, J.A., Handler, M.R., Lorand, J.P., Storey, M., Wainwright, A.N., Luguet, A., Moynier, F., Bizzarro, M. (2017) Late accretion history of the terrestrial planets inferred from platinum stable isotopes. *Geochemical Perspectives Letters* 3, 94–104.

Dale, C.W., Kruijer, T.S., Burton, K.W. (2017) Highly siderophile element and ^{182}W evidence for a partial late veneer in the source of 3.8 Ga rocks from Isua, Greenland. *Earth and Planetary Science Letters* 458, 394–404.

Fischer-Gödde, M., Becker, H. (2012) Osmium isotope and highly siderophile element constraints on ages and nature of meteoritic components in ancient lunar impact rocks. *Geochimica et Cosmochimica Acta* 77, 135–156.

Fischer-Gödde, M., Kleine, T. (2017) Ruthenium isotopic evidence for an inner Solar System origin of the late veneer. *Nature* 541, 525–527.

Fischer-Gödde, M., Elfers, B.M., Münker, C., Szilas, K., Maier, W.D., Messling, N., Morishita, T., Van Kranendonk, M., Smithies, H. (2020) Ruthenium isotope vestige of Earth's pre-late-veneer mantle preserved in Archaean rocks. *Nature* 579, 240–244.

Greenwood, R.C., Barrat, J.A., Miller, M.F., Anand, M., Dauphas, N., Franchi, I.A., Sillard, P., Starkey, N.A. (2018) Oxygen isotopic evidence for accretion of Earth's water before a high-energy Moon-forming giant impact. *Science Advances* 4, 5928.

Herwartz, D., Pack, A., Friedrichs, B., Bischoff, A. (2014) Identification of the giant impactor Theia in lunar rocks. *Science* 344, 1146–1150.

Mattey, D., Lowry, D., Macpherson, C. (1994) Oxygen isotope composition of mantle peridotite. *Earth and Planetary Science Letters* 128, 231–241.

Nishio, I., Morishita, T., Szilas, K., Pearson, G., Tani, K.I., Tamura, A., Harigane, Y., Guotana, J.M. (2019) Titanian clinohumite-bearing peridotite from the ulamertoq ultramafic body in the 3.0 Ga akia terrane of southern west Greenland. *Geosciences* 9, 153.

Palme, H., O'Neill, H. (2003) 2.01 – Cosmochemical estimates of mantle composition. In: Holland, H.D., Turekian, K.K. (Eds.) *Treatise on Geochemistry.* First Edition, Elsevier, Oxford. 1–38.

Peters, S.T.M., Szilas, K., Sengupta, S., Kirkland, C.L., Garbe-Schönberg, D., Pack, A. (2020) >2.7 Ga metamorphic peridotites from southeast Greenland record the oxygen isotope composition of Archean seawater. *Earth and Planetary Science Letters* 544, 116331.

Reimink, J.R., Chacko, T., Carlson, R.W., Shirey, S.B., Liu, J., Stern, R.A., Bauer, A.M., Pearson, D.G., Heaman, L.M. (2018) Petrogenesis and tectonics of the Acasta Gneiss Complex derived from integrated petrology and ^{142}Nd and ^{182}W extinct nuclide-geochemistry. *Earth and Planetary Science Letters* 494, 12–22.

Rumble, D., Bowring, S., Iizuka, T., Komiya, T., Lepland, A., Rosing, M.T., Ueno, Y. (2013) The oxygen isotope composition of earth's oldest rocks and evidence of a terrestrial magma ocean. *Geochemistry, Geophysics, Geosystems* 14, 1929–1939.

Sengupta, S., Pack, A. (2018) Triple oxygen isotope mass balance for the Earth's oceans with application to Archean cherts. *Chemical Geology* 495, 18–26.

Szilas, K., Kelemen, P.B., Bernstein, S. (2015) Peridotite enclaves hosted by Mesoarchaean TTG-suite orthogneisses in the Fiskefjord region of southern West Greenland. *GeoResJ* 7, 22–34.

Valley, J.W., Cavosie, A.J., Ushikubo, T., Reinhard, D.A., Lawrence, D.F., Larson, D.J., Clifton, P.H., Kelly, T.F., Wilde, S.A., Moser, D.E., Spicuzza, M.J. (2014) Hadean age for a post-magma-ocean zircon confirmed by atom-probe tomography. *Nature Geoscience* 7, 219–223.

van de Löcht, J., Hoffmann, J.E., Li, C., Wang, Z., Becker, H., Rosing, M.T., Kleinschrodt, R., Münker, C. (2018) Earth's oldest mantle peridotites show entire record of late accretion. *Geology* 46, 199–202.

Varas-Reus, M.I., König, S., Yierpan, A., Lorand, J.P., Schoenberg, R. (2019) Selenium isotopes as tracers of a late volatile contribution to Earth from the outer Solar System. *Nature Geoscience* 12, 779–782.

Walker, R.J. (2009) Highly siderophile elements in the Earth, Moon and Mars: Update and implications for planetary accretion and differentiation. *Chemie der Erde* 69, 101–125.

Wang, Z., Becker, H. (2013) Ratios of S, Se and Te in the silicate Earth require a volatile-rich late veneer. *Nature* 499, 328–331.

Willbold, M., Elliott, T., Moorbath, S. (2011) The tungsten isotopic composition of the Earth's mantle before the terminal bombardment. *Nature* 477, 195–198.

Young, E.D., Kohl, I.E., Warren, P.H., Rubie, D.C., Jacobson, S.A., Morbidelli, A. (2016) Oxygen isotopic evidence for vigorous mixing during the Moon-forming giant impact. *Science* 351, 493–496.

Geochemical Perspectives Letters

Tight bounds on missing late veneer in early Archean peridotite from triple oxygen isotopes

S.T.M. Peters, M.B. Fischer, A. Pack, K. Szilas, P.W.U. Appel, C. Münker, L. Dallai, C.S. Marien

Supplementary Information

The Supplementary Information includes:

- S-1. Sample Suite
- S-2. Analytical Methods
- S-3. Determining the Bulk Silicate Earth $\Delta'^{17}O$ Value
- S-4. Mass Balance Calculations for Missing Late Veneer
- Figure S-1
- Tables S-1 to S-3
- Supplementary Information References

S-1. Sample Suite

We determined the triple oxygen isotope compositions of olivine from a suite of post-Archean, off-cratonic spinel lherzolite xenoliths, with the exceptions of samples from Hawaii and Beni Boussera, which are dunites. The majority of samples were erupted in continental intraplate magmas, with some samples having erupted in continental rift settings. We studied xenoliths from the East-African Rift system (Great Rift Valley, Ethiopia), the European Cenozoic Rift System (French Massif Central, West Eifel, Hessian Graben, Vogelsberg volcanic field, Ohře/Eger Graben), the Rio Grande Rift (Potrillo Volcanic Field, USA), the Middle Atlas mountains, (Tafraout maar, Morocco), the West Antarctic Rift (Mt. Melbourne volcanic field), and the Eastern block of the North China craton (Changle volcano). In order to investigate whether $\Delta'^{17}O$ values of

subcontinental lithospheric mantle peridotite could potentially have been affected by metasomatic processes or processes of re-fertilisation, we also determined the triple oxygen isotope composition of a peridotite xenolith from the Dariganga volcanic plateau, Mongolia (sample 8520-12), that was previously reported to have a $\delta^{18}O_{ol}$ value of 5.50 ± 0.09 ‰ (Wiechert *et al.*, 1997), *i.e.* a higher $\delta^{18}O_{ol}$ value than typical mantle peridotite ($\delta^{18}O_{ol} \approx 5.2$ ‰). We did not reproduce the elevated $\delta^{18}O_{ol}$ value for this sample, and measured a $\delta^{18}O_{ol}$ of 5.15 ± 0.06 ‰ (Table S-1). A sample of orogenic peridotite from the Beni Boussera lherzolite massif in Morocco (14BB2) was included in the sample suite well. Samples from the suboceanic lithospheric mantle were also measured, and include peridotite xenoliths that were erupted in ocean island basalts (OIBs) from Hawaii (Hualālai volcano), Lanzarote, and Tenerife.

We then determined the triple oxygen isotope compositions of olivine in Archean peridotite, predominantly of dunite composition, from the ultramafic enclaves in the Itsaq Gneiss Complex (IGC) and Fiskefjord region of southwest Greenland. We studied peridotite samples from two localities in the >3.7 Ga Isua supracrustal belt (ISB) (Dymek *et al.*, 1988; Friend *et al.*, 2002; Friend and Nutman, 2011), one locality south of the Isua supracrustal belt (SOISB; Bennett *et al.*, 2002; Friend *et al.*, 2002; van de Löcht *et al.*, 2020), the ~3.8 Ga Narssaq ultramafic body (NUB; Nutman *et al.*, 2007; van de Löcht *et al.*, 2020), and the ~3.8 Ga Ujaragssuit Nunât ultramafic body (Rollinson, 2002; Lowry *et al.*, 2003). Each of these ultramafic enclaves carries an s-process Ru excess compared to the BSE (Fischer-Gödde *et al.*, 2020). The samples from SOISB (10-27, 10-28) and one sample from NUB (10-09) that were analysed in the present study are aliquots of the same samples for which Fischer-Gödde *et al.* (2020) also reported s-process excess Ru. The petrogenesis of these particular samples is discussed in detail by van de Löcht *et al.* (2020). We also determined the triple oxygen isotope compositions of olivine from ultramafic enclaves in the Mesoarchean Fiskefjord region that are geologically related to the Seqi peridotite body (Szilas *et al.*, 2015a), for which excess s-process Ru compared to the bulk silicate Earth was also reported (Fischer-Gödde *et al.*, 2020). Most of the ultramafic enclaves that were studied have been interpreted as slivers of residual mantle peridotite that were entrained in

the Archean crust (Nutman *et al.*, 1996; Bennett *et al.*, 2002; Friend *et al.*, 2002; Rollinson, 2007; van de Löcht *et al.*, 2018, 2020) or, alternatively, as cumulates from (ultra)mafic magmas (*e.g.*, Dymek *et al.*, 1988; Frei *et al.*, 2004; Szilas *et al.*, 2015a, 2015b). The Ujaragssuit Nunât ultramafic body was interpreted as a layered intrusion with intact magmatic layering (Rollinson, 2002).

A common feature of the ultramafic enclaves from the IGC and Fiskefjord region is that forsterite contents in olivine can range up to comparatively high values, with forsterite contents up to 98 mol% reported in samples from the ultramafic lenses of Isua (Friend and Nutman, 2011). Magnetite is often present in the peridotite samples as well, and in some cases the presence of Ti-clinohumite has been reported (Dymek *et al.*, 1988; Friend and Nutman, 2011). These features are in notable agreement with our interpretation that some olivine in the ultramafic enclaves possibly formed by the dehydration of serpentinite minerals (Nishio *et al.*, 2019; Peters *et al.*, 2020). For 3 samples from SOIB and NUB this interpretation is also in line with disturbed internal ^{87}Rb-^{87}Sr and ^{147}Sm-^{143}Nd isochrons, which suggest multiple overprints by fluids for these particular samples (van de Löcht, 2019).

S-2. Analytical Methods

Hand specimens of rock samples were crushed and sieved in different grain size fractions, such that inclusion-free, alteration-free olivine grains could be hand-picked under a binocular microscope for analysis. The samples were reacted with excess BrF_5 in a stainless-steel sample chamber at a pressure of *ca*. 120 mbar, using a laser for heating of the samples. The equivalent sample mass of ~30 μmol O_2 (*i.e.* 2.0–2.2 mg olivine) was reacted, meaning that a single extraction of O_2 typically comprised one to four olivine grains for samples of mantle peridotite xenoliths and five to ten olivine grains for samples of the Archean ultramafic enclaves in southwest Greenland. The O_2 that was released from the samples was cleaned from contaminant gases in a vacuum line using liquid nitrogen-based cooling techniques, NaCl, and a Hewlett Packard 5890 Series II gas chromatograph at 50 °C (Pack *et al.*, 2016; Peters *et al.*, 2020). Most of this cleaning procedure had been

automated and was PC-operated using LabView™. After cleaning the sample gas, it was transferred into a cold trap with 5 Å molecular sieve beads, using a He stream at a flowrate of 10 mL min^{-1}. After He was evacuated from this trap, the sample was expanded into a bellow of a ThermoFinnigan™ MAT253 gas source mass spectrometer by heating the trap in a water bath at 50 °C. The $\delta^{17}O$ and $\delta^{18}O$ values of the samples were then determined by measuring O_2^+ ions at m/z = 32, 33, and 34 for ~40 minutes relative to a reference gas that was calibrated against the VSMOW2 and SLAP2 water standards (Pack *et al.*, 2016).

The triple oxygen isotope compositions of the samples are reported here relative to the composition of San Carlos olivine. Analytical sessions typically comprised measurements of eight samples that were bracketed by a total of six measurements of San Carlos olivine for each individual session. Two different fractions of San Carlos olivine were used for bracketing throughout the course of this study. These two fractions have identical $\Delta'^{17}O$ values at the level of <1 ppm, but have apparently different $\delta^{18}O$ values: One fraction (Göttingen internal ID: 0215M) has a long-term $\delta^{18}O$ value of 5.18 ± 0.01 ‰ (n = 52) whereas the other fraction (Göttingen internal ID: 0919) has a long-term $\delta^{18}O$ value 5.34 ± 0.01 ‰ (n = 91) relative to the composition of UWG-2 garnet ($\delta^{18}O$ = 5.74 ‰; Valley *et al.*, 1995). The samples were normalised to the $\Delta'^{17}O$ value of San Carlos olivine of −51.8 ppm, which is the average value for San Carlos olivine from the studies by Pack *et al.* (2016), Sharp *et al.* (2018), and Wostbrock *et al.* (2020).

S-3. Determining the Bulk Silicate Earth $\Delta'^{17}O$ Value

The $\Delta'^{17}O$ of the bulk silicate Earth (BSE) was previously determined by Herwartz *et al.* (2014; with data from Pack and Herwartz, 2014), Greenwood *et al.* (2018; with data from Starkey *et al.*, 2016), and Cano *et al.* (2020) with precisions of up to ca. 2–3 ppm (1 s.d.) relative to the composition of San Carlos olivine. Some of the samples that were included in these previous studies, however, possibly do not have representative $\Delta'^{17}O$ values for the BSE. Greenwood *et al.* (2018) and Cano *et al.* (2020) included in their studies a number

of glasses and phenocrysts from mid-ocean ridge basalts. However, mid-ocean ridge basalts contain on average 2 % oxygen from subducted, altered oceanic crust and sediments with $\delta^{18}O$ values of ~10.5 ‰ (Eiler *et al.*, 2000). The $\Delta'^{17}O$ values of high-$\delta^{18}O$ altered oceanic crust and sediments are several tens of ppm lower than fertile mantle peridotite (Sengupta and Pack, 2018), implying that the $\Delta'^{17}O$ values of MORB can potentially be lower than fertile mantle peridotite at the <5 ppm level. Greenwood *et al.* (2018) also included samples from ocean island basalts (OIBs) in their study that were later interpreted to possibly reflect a component of subducted, altered oceanic crust in the mantle sources of the OIB samples (Cao *et al.*, 2019). We propose here that olivine in fertile mantle peridotite is possibly a more representative sample type to determine the $\Delta'^{17}O$ of the BSE than mantle melts. Whereas olivine in mantle peridotite can potentially have exchanged oxygen isotopes with fluids and/or melts in the mantle, the oxygen isotope compositions of those fluids and/or melts would have been buffered by the oxygen isotope composition of mantle olivine (Mattey *et al.*, 1994; Chazot *et al.*, 1997). Indeed, there seems little variation in $\delta^{18}O_{ol}$ values of mantle peridotite, even if mantle peridotite samples are considered that experienced pervasive metasomatism (Mattey *et al.*, 1994; Chazot *et al.*, 1997; Regier *et al.*, 2018).

We focused in our study on the analysis of olivine for multiple reasons. First, in mantle peridotite samples, the oxygen isotope composition of olivine is expected to be less affected by possible processes of mantle metasomatism compared to ortho- and clinopyroxene (Perkins *et al.*, 2006), if any of such effects are present in mantle peridotite at all. In the Archean peridotite samples, we additionally focused on the analysis of hand-picked olivine grains to avoid incipient serpentinisation of the samples from obscuring the measured oxygen isotope compositions. Focusing on the triple oxygen isotopes compositions of olivine had the additional advantage that possible mineral-dependent effects during the analytical procedure (*e.g.*, Young *et al.*, 2016) or hypothesised mineral-specific crystal-chemical effects in $\Delta'^{17}O$ (Kohl *et al.*, 2017) do not affect the conclusions presented here.

S-4. Mass Balance Calculations for Missing Late Veneer

Whereas the precise oxygen isotopic values of the pre-late veneer mantle are unknown, they can be calculated from the suggested $\Delta'^{17}O$ value of the pre-late veneer mantle for an assumed composition of the late veneer. In $\delta^{17}O$ versus $\delta^{18}O$ space, the compositions of the pre-late veneer mantle, the bulk silicate Earth and late veneer plot, by definition, on a mixing line (Fig. S-1a). The slope *m* and intercept *i* of the mixing line can be calculated from the $\delta^{17}O$ and $\delta^{18}O$ values of the bulk silicate Earth (BSE) and late veneer (LV):

$$\delta^{17}O = m\delta^{18}O + i \qquad \text{(Eq. S-1a)}$$

with:

$$m = \frac{\delta^{17}O_{LV} - \delta^{17}O_{BSE}}{\delta^{18}O_{LV} - \delta^{18}O_{BSE}} \qquad \text{(Eq. S-1b)}$$

and

$$i = \delta^{17}O_{LV} - m\,\delta^{18}O_{LV} \qquad \text{(Eq. S-1c)}$$

In linearised triple oxygen isotope space, the pre-late veneer mantle also plots on a line with slope 0.528 and intercept that equals the $\Delta'^{17}O$ of the pre-late veneer mantle (PLVM), in per-mil (Fig. S-1b):

$$1000 \ln\left(\frac{\delta^{17}O}{1000} + 1\right) = 0.528 \times 1000 \ln\left(\frac{\delta^{18}O}{1000} + 1\right) + \frac{\Delta'^{17}O_{PLVM}}{1000} \qquad \text{(Eq. S-2)}$$

The δ values of the pre-late veneer mantle correspond to the point of intersection of these two relations (Fig. S-1), i.e.:

$$0.528\delta'^{18}O_{PLVM} + \frac{\Delta'^{17}O_{PLVM}}{1000} = 1000ln\left[m\, e^{\frac{\delta'^{18}O_{PLVM}}{1000}} - m + \frac{i}{1000} + 1\right] \qquad \text{(Eq. S-3)}$$

Eq. (S-3) cannot be solved algebraically, as it has a linear term on the left versus a logarithmic term on the right side, respectively. Instead, the $\delta'^{18}O$ values of the PLVM can be approximated from Eq. (S-3) using the Newton-Raphson method:

$$\delta'^{18}O_{n+1} = \delta'^{18}O_n - \frac{f_{(\delta'^{18}O_n)}}{f'_{(\delta'^{18}O_n)}} \quad \text{(Eq. S-4)}$$

The $\delta'^{18}O_{PLVM}$ value can be used to determine $\delta^{18}O_{PLVM}$, which in turn allows to calculate the missing oxygen atom fraction from the pre-late veneer mantle for an assumed composition of the late veneer. The missing oxygen atom fraction is given by:

$$f_{MLV} = \frac{\delta^{18}O_{BSE} - \delta^{18}O_{PLVM}}{\delta^{18}O_{LV} - \delta^{18}O_{PLVM}} \times \frac{[O]_{BSE}}{[O]_{LV}} \quad \text{(Eq. S-5)}$$

The concentration of oxygen in late accreted materials was assumed in this study to be similar to CI chondrites (46.5 wt. %), with the bulk silicate Earth having 44.33 wt. % oxygen (Palme and O'Neill, 2003). Missing late veneer is expressed in this study relative to the Earth's mass of 5.972×10^{24} kg, assuming a core mass fraction of 32.5 %.

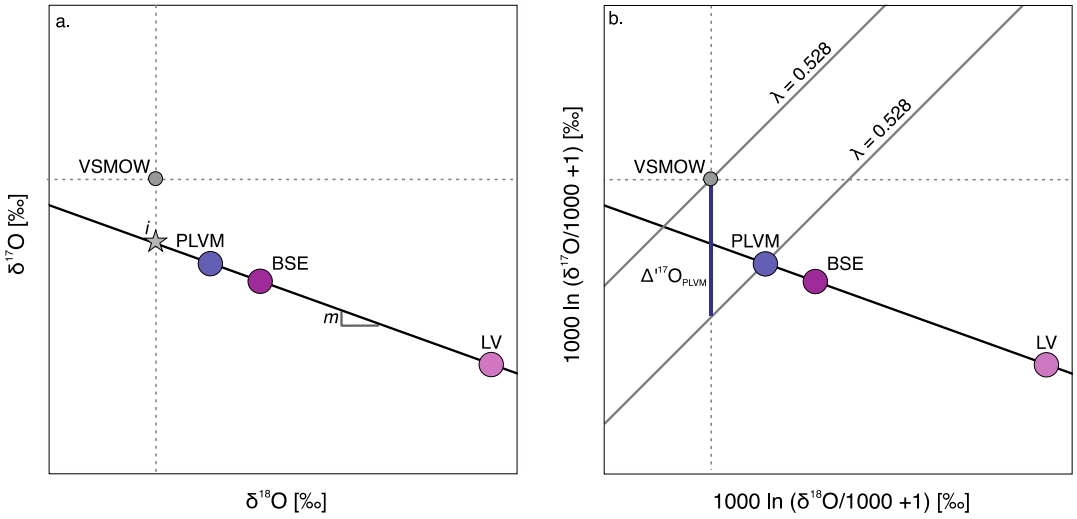

Figure S-1 **(a)** The triple oxygen isotope composition of the pre-late veneer mantle (PLVM) plots in $\delta^{17}O$ versus $\delta^{18}O$ space, by definition, on a mixing line with the compositions of the bulk silicate Earth (BSE) and late veneer (LV). The slope *m* and intercept *i* of the mixing line can be calculated from the triple oxygen isotope compositions of the bulk silicate Earth and an assumed composition for the late veneer (Eq. S-1). **(b)** The triple oxygen isotope composition of the pre-late veneer mantle plots by definition also on a line in $\delta'^{17}O$ versus $\delta'^{18}O$ space with slope $\lambda = 0.528$ and an intercept that equals the $\Delta'^{17}O$ value of the pre-late veneer mantle (Eq. S-2). The point of intersection of Eq. S-1a and Eq. S-2 gives the $\delta^{17}O$ and $\delta^{18}O$ values of the pre-late veneer mantle for an assumed composition of the late veneer.

Using Equations S-1 to S-5, we determined in a Monte Carlo simulation the possible mass of late veneer that can be missing from the early Archean mantle if the missing component had similar compositions to carbonaceous chondrite groups. All carbonaceous chondrite meteorites for which triple oxygen isotope data are available were considered as possible end members for the composition of the late veneer, *i.e.* f_{MLV} was calculated using the oxygen isotope composition of each single meteorite specimen for which data are available (Table S-3). The oxygen isotopic values of the BSE were sampled from a normally distributed data population with $\delta^{18}O = 5.41$ ‰ and $\Delta'^{17}O = -51.6 \pm 2.1$ (1 s.d.). The $\Delta'^{17}O$ value of the pre-late veneer mantle

was sampled from a normally distributed data population as well, using the mean value and standard deviation from this study ($\Delta'^{17}O = -52.3 \pm 1.7$ ppm; 1 s.d.). The 97.72nd percentile of the outcomes of the simulations are considered as the uppermost likely values for missing late veneer.

Supplementary Tables

Table S-1 Triple oxygen isotope compositions of olivine in post-Archean mantle peridotite[1].

Sample ID	Sample locality	Lithology	$\delta^{17}O$ [‰]	±	$\delta^{18}O$ [‰]	±	$\Delta'^{17}O$ [ppm]	±	*n*
Subcontinental lithospheric mantle peridotite									
15koz2	Kozákov volcano, northeast Bohemia (Czech Republic)	sp-lhz	2.73	0.03	5.28	0.06	−53	4	3
31631	Dreiser Weiher maar, Volcanic West Eifel (Germany)	sp-lhz	2.68	0.04	5.18	0.08	−50	4	3
3926-SC3	Hoher Hagen volcanic hill, Hessian graben (Germany)	sp-lhz	2.70	0.06	5.21	0.11	−50	4	3
SP15-VB	Gonterskirchen quarry, Vogelsberg volcanic field (Germany)	sp-lhz	2.68	0.05	5.18	0.09	−54	5	3
SP08-VB	Mont Briançon volcano, French Massif Central (France)	sp-lhz	2.73	0.03	5.27	0.06	−54	4	3
K-L6	Kilbourne hole maar, Potrillo volcanic field (Texas, USA)	sp-lhz	2.76	0.03	5.34	0.06	−52	4	3
8520-12	Atsagin-Dush volcano, Dariganga lava plateau (Mongolia)	sp-lhz	2.66	0.03	5.15	0.06	−53	3	6
TAA31c	Great Rift Valley (Ethiopia)	sp-lhz	2.70	0.03	5.22	0.06	−48	6	3
14MTM1	Tafraout Maar, Azrou volcanic field, Middle Atlas (Morocco)	sp-lhz	2.73	0.04	5.28	0.08	−49	5	2
WR21	Washington Ridge, Mount Melb. volcanic field (Antarctica)	sp-lhz	2.70	0.03	5.22	0.06	−52	4	5
08CL-009	Changle volcano, Shandong province (China)	sp-lhz	2.62	0.04	5.06	0.07	−50	6	2
Orogenic peridotite									
14BB2	Beni Boussera peridotite massif (Morocco)	dn	2.64	0.04	5.10	0.07	−52	5	2
Sub-oceanic lithospheric mantle peridotite									
SP16-LZ-01	Lanzarote, Canary Islands (Spain)	sp-lhz	2.70	0.03	5.21	0.07	−50	4	4
SP16-TF-01	Tenerife, Canary Islands (Spain)	sp-lhz	2.65	0.03	5.13	0.06	−52	4	3
ERG3-33a	Hualālai volcano, Island of Hawai'i (Hawaii, USA)	dn	2.76	0.03	5.34	0.05	−55	5	4
Post-Archean mantle peridotite (mean ± 1 s.d.)			**2.70**	**0.04**	**5.21**	**0.08**	**−51.6**	**2.1**	**15**

[1] $\Delta'^{17}O = 1000\,[\ln(\delta^{17}O/1000 + 1) - 0.528 \times (1000\,\ln(\delta^{18}O/1000 + 1)]$. Sample compositions are expressed relative to the composition of San Carlos olivine with $\Delta'^{17}O = -51.8$ ppm and $\delta^{18}O = 5.17$ ‰ or 5.33 ‰, depending on the San Carlos olivine fraction that was used for bracketing of the samples (see section S-2). Uncertainties for individual samples are given as ±1 s.e.m. for the indicated number n of analyses, whereas mean values are given with uncertainties of ±1 s.d. spl-lhz, spinel lherzolite; dn, dunite.

Table S-2 Triple oxygen isotope compositions of olivine in early Archean peridotite[1] (continues on next page).

Sample ID	Sample locality	Lithology	$\delta^{17}O$ [‰]	±	$\delta^{18}O$ [‰]	±	$\Delta'^{17}O$ [ppm]	±	*n*
Peridotite enclaves in the Itsaq Gneiss Complex (3.8–3.7 Ga)									
194855B	Isua Supracrustal Belt	dn	2.45	0.04	4.74	0.07	−51	5	2
194859	Isua Supracrustal Belt	dn	2.33	0.04	4.52	0.07	−56	5	2
194861	Isua Supracrustal Belt	dn	2.47	0.04	4.79	0.07	−53	5	2
194887A	Isua Supracrustal Belt	dn	2.33	0.04	4.51	0.07	−49	5	2
10-27	South of Isua Supracrustal Belt	dn	2.20	0.04	4.27	0.07	−50	5	2
10-28	South of Isua Supracrustal Belt	dn	2.26	0.03	4.38	0.06	−47	4	3
10-09	Narssaq ultramafic body	dn	1.44	0.03	2.81	0.06	−45	4	3
205065	Narssaq ultramafic body	dn	2.08	0.04	4.05	0.07	−51	8	2
208319	Narssaq ultramafic body	dn	2.24	0.04	4.33	0.07	−46	5	2
479902	Ujaragssuit Nunât	dn	2.46	0.03	4.77	0.06	−50	4	3
479903	Ujaragssuit Nunât	dn	2.34	0.04	4.54	0.07	−52	8	2
479904	Ujaragssuit Nunât	dn	2.69	0.07	5.20	0.13	−54	4	3
479908	Ujaragssuit Nunât	dn	3.19	0.04	6.15	0.07	−48	5	2
479909	Ujaragssuit Nunât	dn	3.23	0.03	6.24	0.06	−59	4	3
479919	Ujaragssuit Nunât	dn	2.50	0.11	4.85	0.21	−51	5	3
479929	Ujaragssuit Nunât	dn	2.51	0.04	4.85	0.07	−47	5	2
479939	Ujaragssuit Nunât	dn	2.41	0.07	4.67	0.13	−52	3	6
Itsaq Gneiss Complex (mean ± 1 s.d.)			2.42	0.40	4.69	0.76	−50.6	3.5	

Table S-2 (continued) Triple oxygen isotope compositions of olivine in early Archean peridotite[1].

Sample ID	Sample locality	Lithology	$\delta^{17}O$ [‰]	±	$\delta^{18}O$ [‰]	±	$\Delta'^{17}O$ [ppm]	±	*n*
Peridotite enclaves in the Fiskefjord region (3.0 Ga)									
482006	Fiskefjord	dn	2.53	0.03	4.88	0.06	−50	4	3
482032	Fiskefjord	dn	2.47	0.03	4.78	0.06	−51	4	3
482033	Fiskefjord	dn	2.73	0.04	5.28	0.07	−49	5	2
482034	Fiskefjord	dn	2.72	0.05	5.25	0.09	−53	4	3
482041	Fiskefjord	dn	2.51	0.03	4.86	0.05	−53	7	4
482054	Fiskefjord	dn	2.43	0.04	4.71	0.07	−54	4	4
Fiskefjord region (mean ± 1 s.d.)			2.56	0.13	4.96	0.24	−51.8	2.0	6
Early Archean mantle (mean ± 1 s.d.)			**2.46**	**0.35**	**4.76**	**0.67**	**−50.9**	**3.2**	**23**
Early Archean mantle (extrapolated ± 1 s.d. to $\delta^{18}O$ = 5.21 ‰)			**2.70**	**0.06**	**5.21**	**0.08**	**−52.3**	**1.7**	**23**

[1] $\Delta'^{17}O = 1000\,[\ln(\delta^{17}O/1000 + 1) - 0.528 \times (1000\ln(\delta^{18}O/1000 + 1)]$. Sample compositions are expressed relative to the composition of San Carlos olivine with $\Delta'^{17}O$ = −51.8 ppm and $\delta^{18}O$ = 5.17 ‰ or 5.33 ‰, depending on the San Carlos olivine fraction that was used for bracketing of the samples (see section S-2). Uncertainties for individual samples are given as ±1 s.e.m. for the indicated number of analyses *n*, whereas mean values are given with uncertainties of ±1 s.d. dn, dunite.

Table S-3 Triple oxygen isotope compositions of chondrites (compilation from the *Meteoritical Bulletin Database*).

Table S-3 is available for download (Excel file) at https://www.geochemicalperspectivesletters.org/article2120.

References

Bennett, V.C., Nutman, A.P., Esat, T.M. (2002) Constraints on mantle evolution from $^{187}Os/^{188}Os$ isotopic compositions of Archean ultramafic rocks from southern West Greenland (3.8 Ga) and Western Australia (3.46 Ga). *Geochimica et Cosmochimica Acta* 66, 2615–2630.

Cano, E.J., Sharp, Z.D., Shearer, C.K. (2020) Distinct oxygen isotope compositions of the Earth and Moon. *Nature Geoscience* 13, 270–274.

Cao, X., Bao, H., Gao, C., Liu, Y., Huang, F., Peng, Y., Zhang, Y. (2019) Triple oxygen isotope constraints on the origin of ocean island basalts. *Acta Geochimica* 38, 327–334.

Chazot, G., Lowry, D., Menzies, M., Mattey, D. (1997) Oxygen isotopic composition of hydrous and anhydrous mantle peridotites. *Geochimica et Cosmochimica Acta* 61, 161–169.

Dymek, R.F., Boak, J.L., Brothers, S.C. (1988) Titanian chondrodite and titanian clinohumite-bearing metadunite from the 3800 Ma Isua supracrustal belt, West Greenland; chemistry, petrology and origin. *American Mineralogist* 73, 547–558.

Eiler, J.M., Schiano, P., Kitchen, N., Stolper, E.M. (2000) Oxygen-isotope evidence for recycled crust in the sources of mid-ocean-ridge basalts. *Nature* 403, 530–534.

Fischer-Gödde, M., Elfers, B.M., Münker, C., Szilas, K., Maier, W.D., Messling, N., Morishita, T., Van Kranendonk, M., Smithies, H. (2020) Ruthenium isotope vestige of Earth's pre-late-veneer mantle preserved in Archaean rocks. *Nature* 579, 240–244.

Frei, R., Polat, A., Meibom, A. (2004) The Hadean upper mantle conundrum: Evidence for source depletion and enrichment from Sm-Nd, Re-Os, and Pb isotopic compositions in 3.71 Gy boninite-like metabasalts from the Isua Supracrustal Belt, Greenland. *Geochimica et Cosmochimica Acta* 68, 1645–1660.

Friend, C.R.L., Bennett, V.C., Nutman, A.P. (2002) Abyssal peridotites >3,800 Ma from southern West Greenland: Field relationships, petrography, geochronology, whole-rock and mineral chemistry of dunite and harzburgite inclusions in the Itsaq Gneiss Complex. *Contributions to Mineralogy and Petrology* 143, 71–92.

Friend, C.R.L., Nutman, A.P. (2011) Dunites from Isua, Greenland: A ca. 3720 Ma window into subcrustal metasomatism of depleted mantle. *Geology* 39, 663–666.

Greenwood, R.C., Barrat, J.A., Miller, M.F., Anand, M., Dauphas, N., Franchi, I.A., Sillard, P., Starkey, N.A. (2018) Oxygen isotopic evidence for accretion of Earth's water before a high-energy Moon-forming giant impact. *Science Advances* 4, 5928.

Herwartz, D., Pack, A., Friedrichs, B., Bischoff, A. (2014) Identification of the giant impactor Theia in lunar rocks. *Science* 344, 1146–1150.

Kohl, I.E., Warren, P.H., Schauble, E.A., Young, E.D. (2017) Limitations on $\Delta'^{17}O$ as a tracer of provenance revealed by mineral specific values from lunar and terrestrial anorthosites. *Lunar and Planetary Science Conference No. 1964*, 2292.

Lowry, D., Appel, P.W.U., Rollinson, H.R. (2003) Oxygen isotopes of an Early Archaean layered ultramafic body, southern West Greenland: Implications for magma source and post-intrusion history. *Precambrian Research* 126, 273–288.

Mattey, D., Lowry, D., Macpherson, C. (1994) Oxygen isotope composition of mantle peridotite. *Earth and Planetary Science Letters* 128, 231–241.

Nishio, I., Morishita, T., Szilas, K., Pearson, G., Tani, K.I., Tamura, A., Harigane, Y., Guotana, J.M. (2019) Titanian clinohumite-bearing peridotite from the ulamertoq ultramafic body in the 3.0 Ga akia terrane of southern west Greenland. *Geosciences (Switzerland)* 9, 153.

Nutman, A.P., Friend, C.R.L., Horie, K., Hidaka, H. (2007) Chapter 3.3 The Itsaq Gneiss Complex of

Southern West Greenland and the Construction of Eoarchaean Crust at Convergent Plate Boundaries. In: van Kranendonk, M.J., Smithies, R.H., Bennett, V.C. (Eds.) *Developments in Precambrian Geology 15: Earth's Oldest Rocks*. Elsevier, Amsterdam, 187–218.

Nutman, A.P., McGregor, V.R., Friend, C.R.L., Bennett, V.C., Kinny, P.D. (1996) The Itsaq Gneiss Complex of southern West Greenland; the world's most extensive record of early crustal evolution (3900–3600 Ma). *Precambrian Research* 78, 1–39.

Pack, A., Herwartz, D. (2014) The triple oxygen isotope composition of the Earth mantle and understanding $\Delta^{17}O$ variations in terrestrial rocks and minerals. *Earth and Planetary Science Letters* 390, 138–145.

Pack, A., Tanaka, R., Hering, M., Sengupta, S., Peters, S., Nakamura, E. (2016) The oxygen isotope composition of San Carlos olivine on the VSMOW2-SLAP2 scale. *Rapid Communications in Mass Spectrometry* 30, 1495–1504.

Palme, H., O'Neill, H. (2003) 2.01 – Cosmochemical estimates of mantle composition. In: Holland, H.D., Turekian, K.K. (Eds.) *Treatise on Geochemistry*. First Edition, Elsevier, Oxford. 1–38..

Perkins, G.B., Sharp, Z.D., Selverstone, J. (2006) Oxygen isotope evidence for subduction and rift-related mantle metasomatism beneath the Colorado Plateau-Rio Grande rift transition. *Contributions to Mineralogy and Petrology* 151, 633.

Peters, S.T.M., Szilas, K., Sengupta, S., Kirkland, C.L., Garbe-Schönberg, D., Pack, A. (2020) >2.7 Ga metamorphic peridotites from southeast Greenland record the oxygen isotope composition of Archean seawater. *Earth and Planetary Science Letters* 544, 116331.

Regier, M.E., Miškovi, A., Ickert, R.B., Pearson, D.G., Stachel, T., Stern, R.A., Kopylova, M. (2018) An oxygen isotope test for the origin of Archean mantle roots. *Geochemical Perspectives Letters* 9, 6–10.

Rollinson, H. (2002) A Metamorphosed, Early Archaean Chromitite from West Greenland: Implications for the Genesis of Archaean Anorthositic Chromitites. *Journal of Petrology* 43, 2143–2170.

Rollinson, H. (2007) Recognising early Archaean mantle: A reappraisal. *Contributions to Mineralogy and Petrology* 154, 241–252.

Sengupta, S., Pack, A. (2018) Triple oxygen isotope mass balance for the Earth's oceans with application to Archean cherts. *Chemical Geology* 495, 18–26.

Sharp, Z.D., Wostbrock, J.A.G., Pack, A. (2018) Mass-dependent triple oxygen isotope variations in terrestrial materials. *Geochemical Perspectives Letters* 7, 27–31.

Starkey, N.A., Jackson, C.R.M., Greenwood, R.C., Parman, S., Franchi, I.A., Jackson, M., Fitton, J.G., Stuart, F.M., Kurz, M., Larson, L.M. (2016) Triple oxygen isotopic composition of the high-$^{3}He/^{4}He$ mantle. *Geochimica et Cosmochimica Acta* 176, 227–238.

Szilas, K., Kelemen, P.B., Bernstein, S. (2015a) Peridotite enclaves hosted by Mesoarchaean TTG-suite orthogneisses in the Fiskefjord region of southern West Greenland. *GeoResJ* 7, 22–34.

Szilas, K., Kelemen, P.B., Rosing, M.T. (2015b) The petrogenesis of ultramafic rocks in the 3.7 Ga Isua supracrustal belt, southern West Greenland: Geochemical evidence for two distinct magmatic cumulate trends. *Gondwana Research* 28, 565–580.

Valley, J.W., Kitchen, N., Kohn, M.J., Niendorf, C.R., Spicuzza, M.J. (1995) UWG-2, a garnet standard for oxygen isotope ratios: Strategies for high precision and accuracy with laser heating. *Geochimica et Cosmochimica Acta* 59, 5223–5231.

van de Löcht, J. (2019) *Geochemistry and petrology of ~3.8 Ga mafic-ultramafic enclaves in the Itsaq Gneiss Complex, SW Greenland*. PhD thesis, Universität zu Köln, 208 pp.

van de Löcht, J., Hoffmann, J.E., Li, C., Wang, Z., Becker, H., Rosing, M.T., Kleinschrodt, R., Münker, C. (2018) Earth's oldest mantle peridotites show entire record of late accretion. *Geology* 46, 199–202.

van de Löcht, J., Hoffmann, J.E., Rosing, M.T., Sprung, P., Münker, C. (2020) Preservation of Eoarchean

mantle processes in ~3.8 Ga peridotite enclaves in the Itsaq Gneiss Complex, southern West Greenland. *Geochimica et Cosmochimica Acta* 280, 1–25.

Wiechert, U., Ionov, D.A., Wedepohl, K.H. (1997) Spinel peridotite xenoliths from the Atsagin-Dush volcano, Dariganga lava plateau, Mongolia: A record of partial melting and cryptic metasomatism in the upper mantle. *Contributions to Mineralogy and Petrology* 126, 345–364.

Wostbrock, J.A.G., Cano, E.J., Sharp, Z.D. (2020) An internally consistent triple oxygen isotope calibration of standards for silicates, carbonates and air relative to VSMOW2 and SLAP2. *Chemical Geology* 533, 119432.

Young, E.D., Kohl, I.E., Warren, P.H., Rubie, D.C., Jacobson, S.A., Morbidelli, A. (2016) Oxygen isotopic evidence for vigorous mixing during the Moon-forming giant impact. *Science* 351, 493–496.